A polyether biotoxin binding site on the lipid-exposed face of the pore domain of Kv channels revealed by the marine toxin gambierol

Ivan Kopljar[a,1], Alain J. Labro[a,1], Eva Cuypers[b], Henry W. B. Johnson[c], Jon D. Rainier[c], Jan Tytgat[b], and Dirk J. Snyders[a,2]

[a]Laboratory for Molecular Biophysics, Physiology, and Pharmacology, University of Antwerp, 2610 Antwerp, Belgium; [b]Laboratory for Toxicology, University of Leuven Campus Gasthuisberg, 3000 Leuven, Belgium; and [c]Department of Chemistry, University of Utah, Salt Lake City, UT 84112-0850

Edited by Christopher Miller, Brandeis University, Waltham, MA, and approved April 24, 2009 (received for review December 8, 2008)

Gambierol is a marine polycyclic ether toxin belonging to the group of ciguatera toxins. It does not activate voltage-gated sodium channels (VGSCs) but inhibits Kv1 potassium channels by an unknown mechanism. While testing whether Kv2, Kv3, and Kv4 channels also serve as targets, we found that Kv3.1 was inhibited with an IC_{50} of 1.2 ± 0.2 nM, whereas Kv2 and Kv4 channels were insensitive to 1 μM gambierol. Onset of block was similar from either side of the membrane, and gambierol did not compete with internal cavity blockers. The inhibition did not require channel opening and could not be reversed by strong depolarization. Using chimeric Kv3.1–Kv2.1 constructs, the toxin sensitivity was traced to S6, in which T427 was identified as a key determinant. In Kv3.1 homology models, T427 and other molecular determinants (L348, F351) reside in a space between S5 and S6 outside the permeation pathway. In conclusion, we propose that gambierol acts as a gating modifier that binds to the lipid-exposed surface of the pore domain, thereby stabilizing the closed state. This site may be the topological equivalent of the neurotoxin site 5 of VGSCs. Further elucidation of this previously undescribed binding site may explain why most ciguatoxins activate VGSCs, whereas others inhibit voltage-dependent potassium (Kv) channels. This previously undescribed Kv neurotoxin site may have wide implications not only for our understanding of channel function at the molecular level but for future development of drugs to alleviate ciguatera poisoning or to modulate electrical excitability in general.

ciguatera | neurotoxin site 5 | polycyclic ether toxin | potassium channels | Kv3.1

Gambierol is a polycyclic ether toxin produced by the marine dinoflagellate *Gambierdiscus toxicus* and belongs to the ciguatoxins (CTXs) that accumulate throughout the food chain. Consumption of contaminated fish causes ciguatera fish poisoning characterized by gastrointestinal and neurological symptoms and by hypotension, bradycardia, respiratory difficulties, and paralysis in severe cases (1).

In general, CTXs are potent toxins of voltage-gated sodium channels (VGSCs), with affinities in the nanomolar range (1, 2). Their mechanism of action includes (*i*) a hyperpolarizing shift in the voltage dependence of channel activation causing channel opening at resting membrane potentials and (*ii*) disruption of the inactivation resulting in persistent activation (3). In contrast to other CTXs, gambierol itself does not affect VGSCs but antagonizes CTX effects on VGSCs at concentrations >100 nM (4). Gambierol does block a potassium current in mouse taste cells (5), and members of the Kv1 subfamily of voltage-dependent potassium (Kv) channels have recently been identified as high-affinity targets (6).

Given these effects on the Kv1 subfamily, we tested whether other Kv subfamilies would be sensitive to gambierol. We found that gambierol inhibited Kv3 channels with nanomolar affinity, whereas Kv2 and Kv4 channels were insensitive. Established mechanisms of Kv channel inhibition include external pore block (e.g., dendrotoxin), internal pore block (open channel block), and gating modification [depolarizing shifts of channel activation by voltage sensor toxins (e.g., hanatoxin)] (3, 7). Our results for gambierol inhibition of Kv3.1 channels did not fit any of these mechanisms. Taking advantage of the subfamily selectivity, we created chimeric constructs between Kv2.1 and Kv3.1 to determine the channel region(s) responsible for the toxin sensitivity, followed by further substituting specific residues to elucidate the molecular determinants for high-affinity inhibition. The results indicate that gambierol probably acts as a gating modifier that stabilizes the closed state of Kv3.1 channels via a previously undescribed binding site that is located outside the permeation pathway.

Results

Potent Kv3.1 Inhibition by Gambierol. Because gambierol is a potent blocker of *Shaker*-type Kv1 channels (6), we tested its effects on members of other Kv subfamilies [Fig. 1 and Fig. S1]. Application of 1 μM gambierol had no effect on Kv2 or Kv4 channels (Fig. 1*A*) but fully suppressed Kv3.1 currents. As a control, we applied 100 nM gambierol to Kv1.4 and observed 66 ± 10% inhibition (n = 3) (Fig. S1), which is comparable to results obtained in *Xenopus* oocytes (6). Fig. 1*B* shows that Kv3.1 channels were already inhibited by 1 nM gambierol, and the concentration dependence of inhibition could be fitted with a Hill equation indicating an apparent affinity IC_{50} of 1.2 ± 0.2 nM and a Hill coefficient n_H of 0.90 ± 0.06 (n = 4–9) (Fig. 1*C*).

Channel inhibition by voltage-sensor toxins such as hanatoxin can be overcome by strong depolarizations in the continuous presence of high toxin concentrations (>50 times the apparent K_d) (7–9). However, 250-ms depolarizations up to +140 mV did not reveal any activation of Kv3.1 currents in the presence of 100 nM gambierol (Fig. 1*D*).

Sidedness of Action. To estimate the kinetics of block development, we monitored the onset of inhibition of Kv3.1 currents during 250-ms steps to +40 mV repeated every 5 s (Fig. 2*A* and *C*). During the application of 100 nM gambierol, the maximum currents displayed an exponential decay with a time constant of 65 ± 10 s (n = 11) or a rate λ of 0.015 s^{-1}, reaching complete inhibition within 4 min. Recovery from block was slow and reached only 10–15% after 5 min of washout. In the case of a bimolecular interaction, the apparent on- and off-rate constants k and l, respectively, can be

Author contributions: I.K., A.J.L., J.T., and D.J.S. designed research; I.K. and A.J.L. performed research; H.W.B.J. and J.D.R. contributed new reagents/analytic tools; I.K., A.J.L., and E.C. analyzed data; and I.K., A.J.L., and D.J.S. wrote the paper.

The authors declare no conflict of interest.

This article is a PNAS Direct Submission.

Freely available online through the PNAS open access option.

[1]I.K. and A.J.L. contributed equally to this work.

[2]To whom correspondence should be addressed. E-mail: dirk.snyders@ua.ac.be.

This article contains supporting information online at www.pnas.org/cgi/content/full/0812471106/DCSupplemental.

www.pnas.org/cgi/doi/10.1073/pnas.0812471106

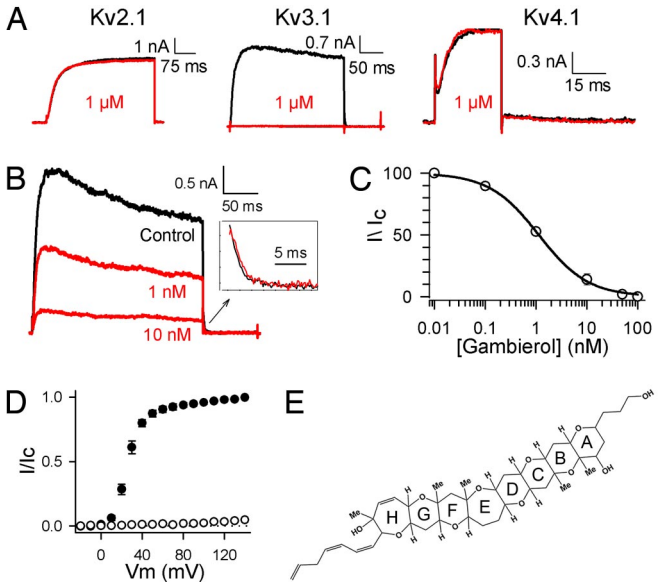

Fig. 1. Potent Kv3.1 inhibition by gambierol. (*A*) Current recordings of Kv2.1, Kv3.1, and Kv4.1 elicited by a depolarizing step to +40 mV from a holding potential of −80 mV for Kv2 and Kv3 channels or −90 mV for Kv4 channels. Raw current traces were leak corrected, and scale bars are given (*Inset*). Note that the current recordings before (black) and after (red) application of 1 μM gambierol were similar for Kv2.1 and Kv4.1, whereas Kv3.1 was completely inhibited. (*B*) Typical current recordings at +40 mV under control conditions (black trace) and after application of 1 and 10 nM gambierol (red traces). (*Inset*) Superposition of the scaled tail currents at −40 mV in control and after application of 1 nM gambierol showing similar decay kinetics. (*C*) Concentration dependence of Kv3.1 inhibition by gambierol obtained from the normalized current suppression (from recordings as in *B*) as a function of the gambierol concentration, fitted with the Hill equation (solid line). (*D*) Voltage-dependence of Kv3.1 activation from the normalized tail currents at −40 mV after 250-ms activating steps to potentials between −20 and +140 mV, for control (filled circles) and after application of 100 nM gambierol (open circles) ($n = 4$). The dashed line represents the 0 current level. (*E*) Structure of gambierol showing the 8-ring structure (A–H) of the polycyclic ether toxin.

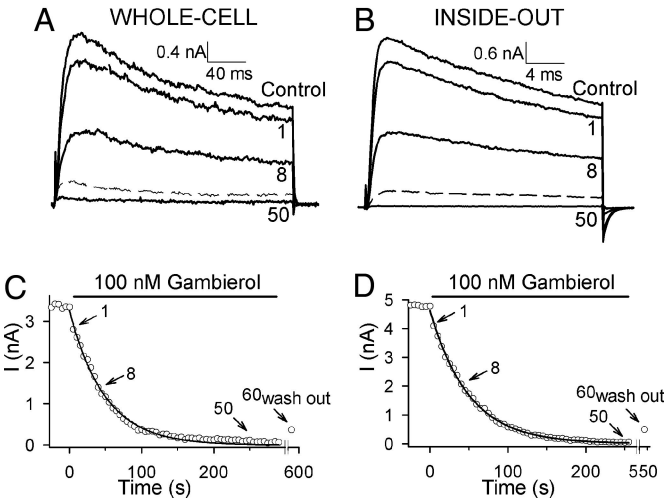

Fig. 2. Onset of gambierol inhibition in whole-cell and inside-out configurations. (*A*) Kv3.1 current recordings in the whole-cell configuration elicited by a train of 250-ms steps to +40 mV, applied every 5 s. Shown are the control trace; the first, eighth, and 50th traces with application of 100 nM gambierol (solid lines); and the 60th trace of the washout (dashed line). Note the slow recovery of only ≈15% after the 300-s washout. (*B*) Kv3.1 current recordings in inside-out configuration elicited by a pulse protocol as in *A*. Time course of block in whole-cell (*C*) and inside-out (*D*) configurations with 100 nM gambierol, obtained by plotting the maximum current amplitude from *A* or *B* against time. The solid line illustrates the monoexponential fit with time constants of 49 s (*C*) and 50 s (*D*).

obtained from $\lambda = k[\mathrm{D}] + l$ and $\mathrm{IC}_{50} = l/k$. This yielded values for $k = 0.15 \times 10^6\ \mathrm{M}^{-1}\ \mathrm{s}^{-1}$ and $l = 0.18 \times 10^{-3}\ \mathrm{s}^{-1}$. Consistent with these slow rate constants, an apparent channel inactivation, typical for an open channel blocker, was not observed (Figs. 1*B* and 2*A*).

Because these experiments were done using repetitive pulsing, the inhibition could be attributable to cumulative open state block. To test whether gambierol could block Kv3.1 channels in the closed state, we kept the cells at −80 mV for 4 min (same duration as the pulse train) after the start of 100 nM gambierol perfusion. Fig. 3*A* shows a complete reduction of Kv3.1 current (99.8% ± 0.2 of control, $n = 4$) during the subsequent initial depolarization to +40 mV (equivalent to pulse 48 in Fig. 2*C*), as expected if closed state block proceeded with a time constant <65 s (Fig. 2*C*) during this 4-min interval. Therefore, gambierol inhibition of Kv3.1 channels (*i*) is not use dependent and (*ii*) does not require channel opening.

Because of the highly lipophilic character of gambierol, the toxin might accumulate in the lipid bilayer or cross it to block the channel from the inside. To test for this latter possibility, the onset of block was compared in whole-cell and inside-out configurations. Using the same pulse protocol as in Fig. 2*A*, we observed in the inside-out conditions an exponential decline of the Kv3.1 current with a time constant of 88 ± 15 s ($n = 8$), which was not significantly different from the time constant of 65 s obtained in whole-cell conditions (Fig. 2 *B* and *D*). The similar onset of block from either side of the membrane suggested that gambierol reaches its binding site through a similar path, presumably the lipid bilayer.

To exclude further the presence of gambierol inside the permeation pore, we tested for competition with flecainide, an internal pore blocker (10). We initially applied 10 μM flecainide, which produced a typical time-dependent decline of current during the depolarizing step. After achieving steady state, we applied 1.2 nM (IC_{50}) gambierol in the continued presence of flecainide. Fig. 3*B* shows that this resulted in an additional inhibition of 48.7 ± 4.9% ($n = 4$) compared with the current blocked by 10 μM flecainide alone. The additional ≈50%

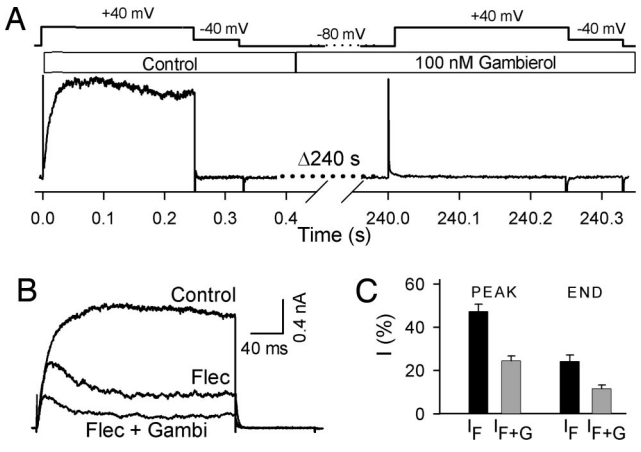

Fig. 3. Closed state inhibition and drug competition. (*A*) Gambierol (100 nM) was applied as in Fig. 2*A*, but the cell was kept at −80 mV for 240 s. The initial depolarizing step with gambierol (corresponding in time to step 48 in 2*C*) shows complete inhibition, indicating that channel opening was not required for inhibition. (*B*) Test for competition between flecainide (Flec) and gambierol (Gambi). Shown are the currents for the 250-ms steps to +40 mV for control, steady-state block by 10 μM Flec, and the subsequent effect of 1.2 nM Gambi together with 10 μM Flec. The latter resulted in an additional block of ≈50% of the Flec-blocked current. (*C*) Reduction of peak and steady-state Kv3.1 currents by flecainide alone, I_F, or combined with gambierol, I_{F+G}.

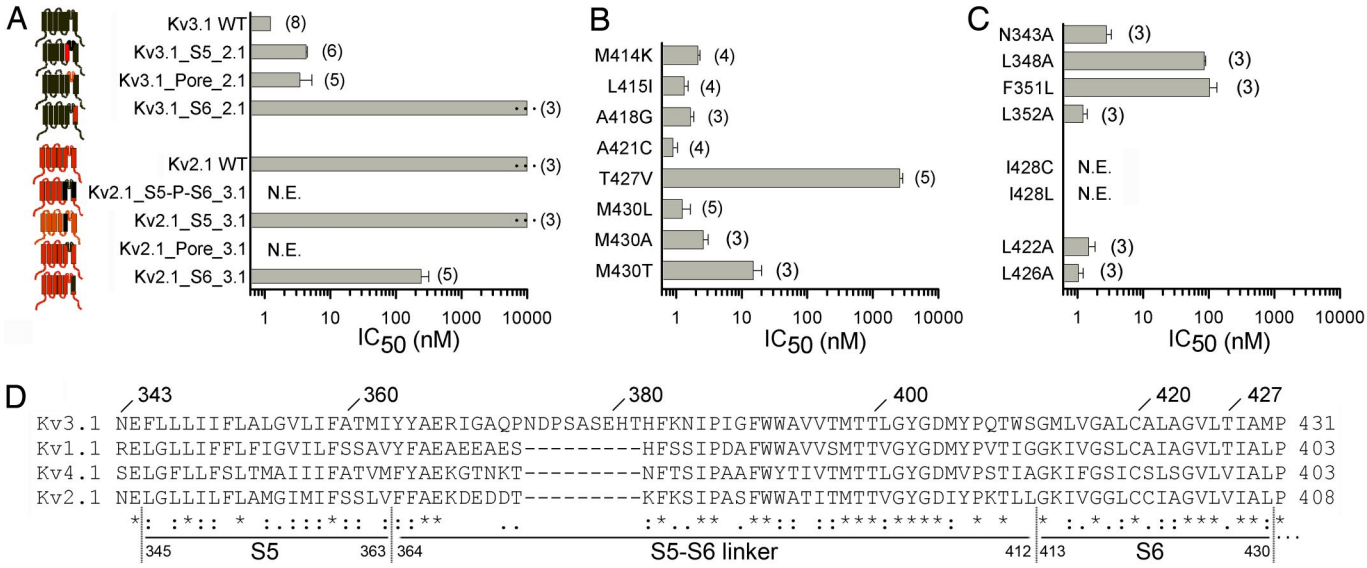

Fig. 4. Molecular determinants of gambierol selectivity. (*A*) Sensitivity of different Kv2.1–Kv3.1 chimeras for gambierol. The IC_{50} values are shown for WT Kv2.1, WT Kv3.1, and the various chimeras. Note that swapping the S5 or the S5–S6 linker (containing the P-loop region) of Kv2.1 into the Kv3.1 background had only a minor effect on the affinity, whereas placing S6 of Kv2.1 in Kv3.1 completely abolished the affinity. Conversely, introduction of S6 from Kv3.1 in a Kv2.1 background resulted in a moderately sensitive channel with an IC_{50} of 245 ± 73 nM. Constructs that were not sensitive to 1 μM gambierol are shown with a dotted line at the end of the bar. (*B*) Substitution of individual S6 residues from Kv2.1 in a Kv3.1 background: only the T427V mutation abolished the high affinity for gambierol. (*C*) Affinities of several additional mutations in S5 and S6 made based on our homology model. (*D*) Sequence alignment of the amino acid residues from S5 to S6 of Kv1.1, Kv2.1, Kv3.1, and Kv4.1 with identity indicated by an asterisk (*) and strong homology by a colon (:). The segments used in the chimeric swaps are indicated with ''S5'', ''S5–S6 linker'', and ''S6'' together with the Kv3.1 numbering.

inhibition indicates that gambierol did not compete for the same binding site as flecainide. Taken together, these results indicate that gambierol does not act as a pore blocker, and therefore interacts with a different binding site that is most likely outside the permeation pathway and accessible in the closed state.

Identification of the Binding Site for Gambierol. To define the potential binding site(s) of gambierol in the Kv3.1 channel, we took advantage of the insensitivity of Kv2.1 subunits (Fig. 1*A*) to create chimeric constructs between the sensitive Kv3.1 and the insensitive Kv2.1 subunits. In the Kv3.1 background, when the complete S5 segment or S5–S6 linker (including the P-loop) was exchanged for the corresponding Kv2.1 sequence, only a small increase in IC_{50} was observed (Fig. 4*A* and Fig. S1). Replacing the S6 segment by the Kv2.1 sequence eliminated high-affinity inhibition, however, because even 1 μM gambierol had no effect (Fig. 4*A*). The opposite exchange resulted in a gambierol-sensitive Kv2.1 chimera that displayed an IC_{50} of 245 ± 73 nM (n = 5) (i.e., intermediate compared with both WT channels) (Fig. 4*A*). Thus, swapping the S6 segment between both channels eliminated the high gambierol sensitivity of Kv3.1 or partly transferred it onto Kv2.1.

Next, we replaced those S6 residues in Kv3.1 that differed from Kv2.1 individually with their Kv2.1 counterpart. These substitution mutants resulted in channels with biophysical properties similar to WT Kv3.1. With the exception of T427V, none of these substitutions affected the toxin sensitivity (Fig. 4*B* and Fig. S2). Interestingly, the replacement of the polar threonine residue at position 427 by a hydrophobic valine fully eliminated high-affinity block in Kv3.1, whereas the biophysical properties of T427V were similar to those of WT (Fig. S3), suggesting that the overall channel structure was preserved. This reduction in affinity was similar whether the toxin was applied from the outside or the inside (Fig. S3). The corresponding substitution in Kv2.1 (V404T) rendered Kv2.1 moderately sensitive to gambierol (IC_{50} = 504 ± 28 nM, n = 3), similar to the complete S6 exchange (Fig. 4*A*). To probe for the physicochemical nature of the interaction between T427 and gambierol, we replaced T427 by a serine, lysine, cysteine, and alanine, thus varying the hydrogen-bonding abilities of the side chain at the 427 position. The rank order for the IC_{50} values was T = S<K<C<A<V (Fig. S3), suggesting that the hydrogen bonding with the side chain at position 427 may be an important determinant for high gambierol affinity. Kv1 subunits also possess a threonine at the site equivalent to T427 in Kv3.1 and are similarly sensitive to gambierol (Fig. S1).

Additional Molecular Determinants in the Binding Site. In both the crystal structure of rKv1.2 (11) (representative of the open state) and in a recent model for the closed state (12), the equivalent residue of T427 (T401 in Kv1.2) faces away from the K^+ permeation pathway and points toward a space between S5 and S6. In combination with our data arguing against gambierol binding in the permeation pathway, this reinforces the possibility of gambierol acting through a previously undescribed binding site that is located outside the channel pore.

To explore this hypothesis, we created hKv3.1 homology models based on the rKv1.2 crystal structure (11) and the Kv1.2 closed state model (12) to identify residues in the vicinity of T427 that would also project into the space between S5 and S6. Both homology models showed that several residues in the S5 segment (L347, L348, and F351) as well as M430 (S6) point toward this space (Fig. 5). To evaluate if reduction of the side-chain volume at these positions affected gambierol sensitivity, we substituted alanine for L347 and L348 and leucine for F351. Both L348A and F351L reduced the affinity by ≈2 orders of magnitude to 86 ± 5 nM (n = 3) and 104 ± 29 nM (n = 3), respectively (Fig. 4), whereas L347A did not affect the high- affinity inhibition. The S6 substitution M430L did not affect the toxin affinity either, but a threonine substitution decreased sensitivity modestly. Mutating I428 (adjacent to T427) to either an alanine or a cysteine yielded no detectable Kv currents, and mutations L422A and L426A (both pointing toward S5 of the adjacent subunit) did not reduce the high affinity for gambierol. Taken together, several

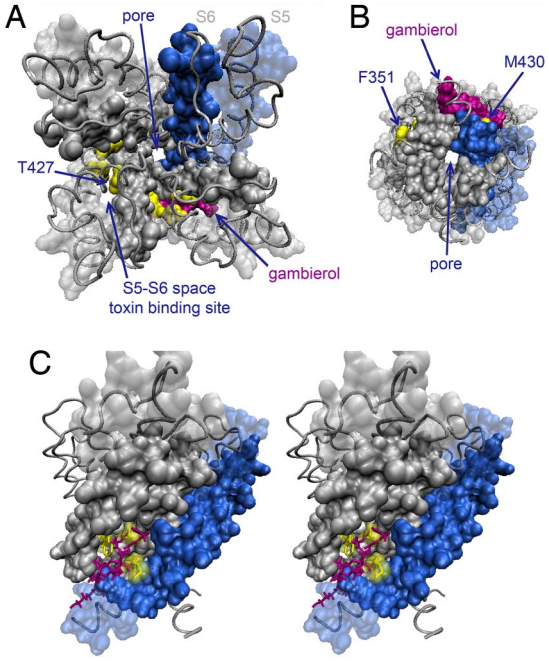

Fig. 5. Homology model for Kv3.1 with gambierol's binding site. Closed state Kv3.1 homology model obtained as detailed in *Materials and Methods*, with the voltage-sensing domain omitted for clarity. (*A*) Top view from the extracellular side on the Kv3.1 channel (gray, with 1 subunit in blue) with 1 gambierol molecule (purple) positioned at its potential binding site. The whole sequence is shown in ribbon representation, whereas for S5 and S6, the solvent-accessible surface is added (transparent in case of S5). The main residues that determine gambierol sensitivity (L348, F351, T427, and M430) are colored yellow. Note that residue T427, which determines high toxin sensitivity, points away from the channel pore and lines a space between the S5 and S6 segments. Because of the 4-fold symmetry, there are 4 such S5–S6 spaces. (*B*) Similar representation as in *A* but now viewed from the internal side, clearly showing gambierol located outside the pore (K^+ permeation pathway). (*C*) Stereo pair of the toxin channel configuration viewed from the membrane (side view). This view highlights the space formed by the lipid-exposed sides of the S5 and S6 segments, which is lined by the important residues (yellow). The size of the space is large enough to accommodate easily a gambierol molecule positioned such that its ladder structure runs roughly parallel to the S5–S6 helices (see also Movie S1).

residues that line the space between S5 and S6 (especially T427, L348, and F351) affected the sensitivity for gambierol when mutated.

Discussion

The main findings of the current study are that gambierol causes potent inhibition of Kv3 channels (*i*) with nanomolar apparent affinity, (*ii*) with slow on- and off-rate constants, (*iii*) in the closed state (or a state-independent manner), and (*iv*) with molecular binding determinants in parts of S5 and S6 that face away from the central cavity. Previously, we reported that the polycyclic ether toxin gambierol did not display Na^+ channel activation (as do other CTXs) but acted as a potent blocker of the Kv1 subfamily (6). Expanding these studies to other traditional Kv channels, we found that even 1 μM gambierol did not affect Kv2 and Kv4 channels, although it inhibited Kv3.1 channels with an IC_{50} of 1.2 nM and a Hill coefficient n_H of 0.9. To determine the mechanism of action, we tested for 3 well-described mechanisms of blocking Kv channels: external pore block, internal cavity (open channel) block, or gating modification (3, 7, 13).

The possibility that gambierol acts as an external pore blocker (e.g., charybdotoxin, dendrotoxin) (14, 15) was examined by swapping the S5–S6 linker between the sensitive Kv3.1 and insensitive Kv2.1 channels. Indeed, previous studies have mapped the binding site of several external blockers such as dendrotoxin or external tetraethylammonium (TEA) to critical residues located in the linker between S5 and S6 that includes the P-loop (15, 16). As a control, we found that the lower TEA sensitivity of Kv2.1 was indeed transferred in this chimera (Fig. S4). However, this chimera retained the high-affinity current inhibition by gambierol (Fig. 4*A*), indicating that this region does not contain residues critical for the different sensitivity of Kv3.1 and Kv2.1. Taken together, these results argue against the possibility of gambierol being an external pore blocker.

A second well-defined mechanism is block through binding in the internal cavity. In this case, channel opening is usually required before the drug can access its binding site (i.e., open channel block). Many local anesthetics, antiarrhythmics, and quaternary ammonium derivatives act in this manner (17, 18). Depending on the interaction rate constants, typical functional observations for open channel block include (*i*) a time-dependent decline of current after activation and (*ii*) a hooked tail configuration and/or tail current crossover reflecting slowed deactivation because the drug must vacate the cavity before the channel can close (foot-in-the-door mechanism) (17–19). However, the calculated on- and off-rate constants of gambierol block were quite slow compared with channel kinetics, precluding such observations, and the tail currents shown in Fig. 1*B Inset* show no evidence for such an effect. The lack of observable kinetic changes does not formally exclude an open channel block mechanism, and it could be argued that the progressively developing block during the pulse trains (Fig. 2*A*) indicated a need for channel opening, as in the case of dofetilide (20). This possibility was excluded by the observation that gambierol inhibition developed on a similar (or perhaps faster) time scale without channel activation (Fig. 3). Finally, competition experiments with an established internal cavity blocker provided no evidence that gambierol competes for the same binding site (Fig. 3 *B* and *C*). Indeed, if 2 drugs do not compete for the same site, addition of the second drug at a concentration corresponding to its IC_{50} should block 50% of the remaining current, as observed (Fig. 3*C*). Similar results were obtained for the interaction with 4-aminopyridine (Fig. S5). Furthermore, the main molecular determinant, T427, does not belong to the set of residues implicated in internal cavity block by various drugs (10, 18, 21).

Hanatoxin is a voltage-sensor toxin that modifies gating of Kv2.1 by interacting with the extracellular part of the voltage sensor, thereby stabilizing the voltage sensor in its resting conformation (7). This increases the rate of channel closure and causes a large positive shift in the voltage dependence of activation, which amounted to ≈50 mV for hanatoxin concentrations of 200 nM to 5 μM (8). Because Fig. 1*D* shows no evidence of Kv3.1 activation at potentials up to +140 mV in the presence of 100 nM gambierol, it follows that gambierol strongly stabilizes the closed state of Kv3.1, because the voltage-dependence is shifted by at least 100 mV. However, the results with the S6 chimeras and the T427 mutants indicate that this gating modification derives from an interaction with a previously undescribed toxin/drug-binding site in Kv channels.

Peptide toxins affect the pore or voltage sensor from the outside and may partition in the extracellular leaflet but have not been shown to target S6 (7, 22, 23). CTXs and brevetoxins (both sharing a similar chemical structure with gambierol) interact with VGSCs at intramembrane neurotoxin site 5 proposed to be formed by the lipid-exposed parts of S6 from domain I and S5 from domain IV (3, 24). These site 5 toxins alter the biophysical properties of the VGSCs by (*i*) shifting the voltage dependence of activation to more hyperpolarizing potentials and (*ii*) inhibiting the inactivation process, both resulting in persistent activation. Thus, these toxins cause a "gain-of-function" through

allosteric modification of Na^+ channel gating (3, 25) (i.e., stabilization of the open state of the channel).

Gambierol does not affect Na^+ channel gating but acts as a functional antagonist of neurotoxin site 5 on VGSCs (3, 4, 26). Therefore, gambierol should also bind at site 5 but apparently lacks the interactions to affect Na^+ channel gating, possibly because it is smaller than the active CTXs. Indeed, gambierol contains only 8 rings (Fig. 1*E*), whereas Na^+ channel site 5-interacting toxins typically have 10 rings or more (e.g., 13 for CTXs) (1, 2). These facts, combined with our data, strongly suggest that the gambierol binding site in Kv3.1 is topologically equivalent to the Na^+ channel neurotoxin site 5. However, the gambierol effect on Kv channels differs in that it strongly stabilizes the closed state of the channel (i.e., it results in a "loss of function").

The facts that gambierol can inhibit closed channels and that the onset of inhibition is independent of the side of application indeed suggest that gambierol reaches its binding site through the plasma membrane, which is compatible with its lipophilic nature (calculated log$P$ = 5.41). Binding at this site would then allosterically block permeation by stabilizing the closed state. In fact, the apparent binding rate constant deduced from the data in Fig. 2 is quite high for a large molecule such as gambierol, but lower and more reasonable estimates are obtained when taking into account the membrane partitioning (see *SI Text*), further supporting a membrane-access mechanism (9, 22).

With chimeric constructs and site-directed mutagenesis, we identified T427 as a key determinant for high-affinity inhibition. It is unlikely that the loss of high-affinity binding in the T427V mutant would be attributable to an allosteric effect from an overall conformational change in channel structure, because the gating properties were similar to WT in both the kinetics and voltage dependence of activation (the difference in Gibbs free energy of activation at 0 mV ($\Delta\Delta G_0$) was only 0.47 kcal/mol; see Fig. S3). Sequence alignment of the S6 segment (Fig. 4*D*) shows that this threonine is conserved in the Kv1 and Kv3 subfamilies, whereas the insensitive Kv2 and Kv4 subfamily members have a valine at this position. Furthermore, replacing T427 in Kv3.1 with an alanine, valine, or cysteine completely abolished the high affinity, whereas the substitution to residues that can form hydrogen bonds (serine, lysine) preserved the high affinity, suggesting that the hydrogen-bonding ability of residue T427 in Kv3.1 is a major determinant of gambierol block.

According to our Kv3.1 homology model that was based on the 3D crystal structure of rKv1.2, this threonine T427 points away from the central cavity and projects into a space between S5 and S6. However, because rKv1.2 was crystallized in the open state, our Kv3.1 homology model most likely also represents the open channel configuration. Because gambierol can block Kv3.1 channels in the closed state, we analyzed the orientation of T427 in a Kv3.1 homology model of a recent model for rKv1.2 in the closed state (12). In this model, T427 still points toward the space between S5 and S6. Fig. 5 shows that this space is large enough to accommodate the gambierol toxin, with its ladder structure roughly parallel to these helices (see also Movie S1). Such an arrangement has previously been proposed for the interaction of other polyether toxins with transmembrane helices (2).

Fig. 5 shows gambierol penetrating this space with its H-ring in the neighborhood of T427 and its hydroxy-propyl end near the cytosol. This orientation was chosen because the H-ring has been shown to be important for the potency of gambierol in mice (27). Further studies are needed to confirm this orientation because other positions are possible. If the hydrogen-bonding ability of T427 determines high-affinity block (Fig. S3), it is conceivable that this involves one of the ether oxygens of gambierol. Furthermore, the S5 residues L348 and F351, which also influence the affinity on mutation, come in proximity to different parts of the gambierol backbone. Taken together, positioning gambierol at this site between the S5 and S6 segments fits quite well with our experimental data. Because of the 4-fold symmetry of a Kv channel, there should be 4 non-overlapping and presumably independent binding sites (Fig. 5). The Hill coefficient of 0.9 therefore suggests that binding of 1 gambierol molecule would be sufficient for inhibition by stabilizing the closed state of at least 1 subunit.

When we attempted to position gambierol in a similar manner in our Kv3.1 homology model of the open state, the space between S5 and S6 was still present, but it was narrower, which resulted in some sterical collisions with gambierol. Obviously, we have to take into account that we used rigid structures and that both the toxin and the channel may adopt slightly different conformations (i.e., induced fit), but a full modeling attempt was beyond the scope of the present study. A more speculative explanation of this poorer fit in the open state is that gambierol binds the channel efficiently in the closed state and subsequently prevents the channels from reaching the open conformation.

Given the nanomolar affinity of Kv3.1 and Kv3.3 (data not shown) for gambierol and the presence of Kv3.x channels in the gastrointestinal tract (28) and in the nervous system (29), Kv3 channels should also be considered likely targets in the pathophysiology of ciguatera intoxication. Further elucidation of this intramembranous polyether binding site in Kv channels may explain why certain ciguatera toxins affect VGSCs, whereas others affect Kv channels. This also raises the question of whether the larger brevetoxins and CTXs (*i*) may also bind to the Kv channels and, if so, (*ii*) whether they would stabilize either the open or closed state. These larger toxins generally do not affect Kv channels (1, 2); if they bind, they are probably too large to fit properly or do not present the required functional group(s) to interact with the (cytoplasmic) gating machinery. Nevertheless, there is a study that reported inhibition of Kv currents in rat dorsal root ganglia neurons by the pacific CTX-1 with an IC_{50} around 20 nM (30).

In conclusion, we propose that gambierol binds at a previously undescribed binding site in Kv channels, which is the topological equivalent of the neurotoxin site 5 of VGSCs. This binding site is located outside the conduction pathway in a space between S5 and S6, with T427 as a major determinant on the lipid-exposed face of these helices. Gambierol binding at this site inhibits K^+ permeation by stabilizing the closed state, contrasting with most CTXs, which affect gating of VGSCs by stabilizing its open state. This unique Kv neurotoxin site may have wide implications not only for our understanding of channel function at the molecular level in its lipid environment but for future development of drugs to modulate electrical excitability (for diseases such as epilepsy, arrhythmias, and chronic pain).

Materials and Methods

Molecular Biology. All Kv channels used were cloned in a EGFP-N1 expression vector. Chimeric Kv2.1/Kv3.1 constructs and single-residue mutants were created using the QuikChange Site-Directed Mutagenesis kit (Stratagene) and mutant primers. Double-strand sequencing confirmed the presence of the desired modification and the absence of unwanted mutations. Plasmid DNA was amplified in XL2 blue script cells (Stratagene) and isolated using the GenElute HP plasmid maxiprep kit (Sigma-Aldrich).

Electrophysiology. Ltk^- cells (mouse fibroblasts, American Type Culture Collection CLL.1.3) were cultured in DMEM with 10% horse serum (vol/vol %) and 1% penicillin/streptomycin. Cells were transiently transfected with 15 ng up to 1 μg of cDNA for WT or mutant constructs using polyethylenimine (Sigma-Aldrich).

Current measurements were done ≈20 h after transfection at room temperature (20–23 °C) with an Axopatch-200B amplifier and were digitized with a Digidata-1200A (Axon Instruments). Command voltages and data storage were controlled with pClamp8 (Axon Instruments) software. Patch pipettes were pulled from 1.2-mm quick-fill borosilicate glass capillaries (World Precision Instruments) with a P-2000 puller (Sutter Instrument Co.) and heat

polished. The bath solution contained 130 mM NaCl, 4 mM KCl, 1.8 mM $CaCl_2$, 1 mM $MgCl_2$, 10 mM Hepes, and 10 mM glucose adjusted to pH 7.35 with NaOH. The pipette solution contained 110 mM KCl, 5 mM K_4BAPTA, 5 mM K_2ATP, 1 mM $MgCl_2$, and 10 mM Hepes adjusted to pH 7.2 with KOH. Junction potentials were zeroed with the filled pipette in the bath solution. For inside-out patches, the pipette was filled with the previous bath solution and the bath was filled with the a solution containing 120 mM KCl, 5 mM K_4BAPTA, and 10 mM Hepes 10 adjusted to pH 7.2 with KOH. Experiments were excluded from analysis if the voltage error estimate based on the size of the current exceeded 5 mV after series resistance compensation.

Gambierol (CAS 146763–62-4) was synthesized as described previously (31), and stock solutions were prepared as 2, 20, and 300 μM in DMSO and diluted with extracellular medium to the appropriate drug concentrations. The final DMSO concentration never exceeded 0.5%, and drug concentrations were applied using a fast perfusion system (ALA Scientific Instruments). Flecainide was obtained from Meda Pharma.

Data Analysis. Details of voltage protocols were adjusted based on the different biophysical properties of the channels. The voltage dependence of activation was fitted with a single Boltzmann equation. Dose-response curves were obtained by plotting y, the fraction of current remaining at +40 mV, as a function of toxin concentration, T, and fitted with the Hill equation $1 - y = 1/(1 + (IC_{50}/[T])^{n_H})$, where IC_{50} is the concentration that generates 50% inhibition and n_H is the Hill coefficient. Results are expressed as mean ± SEM, with n being the number of cells analyzed; error flags are shown if larger than symbol size.

Molecular Models. Kv3.1 homology models were based on the 3D crystal structure of rKv1.2 (Protein Data Bank code 2A79) for the open state (11) and on a recent model of the closed state (12). After aligning the sequence of the S4–S6 region, the Kv3.1 homology models were generated using SWISS-MODEL (32). Illustrations in Fig. 5 were produced with the program Visual Molecular Dynamics (33).

ACKNOWLEDGMENTS. We are grateful to T. De Block for her excellent technical assistance. I.K. is a fellow with the Institute for the Promotion of Innovation through Science and Technology in Flanders. This work was supported by the Interuniversity Attraction Poles program P6/31 of the Belgian Federal Science Policy Office, Research Foundation Flanders (FWO) Grants G025708 (to D.J.S.) and G033006 (to J.T.), special research fund (BOF) Grants TOP22293 (to D.J.S.) and OT-05–64 (to J.T.), and National Institutes of Health Grant GM56677 (to J.D.R.).

1. Nicholson GM, Lewis RJ (2006) Ciguatoxins: Cyclic polyether modulators of voltage-gated ion channel function. *Marine Drugs* 4:82–118.
2. Nicolaou KC, Frederick MO, Aversa RJ (2008) The continuing saga of the marine polyether biotoxins. *Angew Chem Int Ed* 47:7182–7225.
3. Catterall WA, Cestele S, Yarov-Yarovoy V, Yu FH, Konoki K, et al. (2007) Voltage-gated ion channels and gating modifier toxins. *Toxicon* 49:124–141.
4. Lepage KT, Rainier JD, Johnson HW, Baden DG, Murray TF (2007) Gambierol acts as a functional antagonist of neurotoxin site 5 on voltage-gated sodium channels in cerebellar granule neurons. *J Pharmacol Exp Ther* 323:174–179.
5. Ghiaroni V, et al. (2005) Inhibition of voltage-gated potassium currents by gambierol in mouse taste cells. *Toxicol Sci* 85:657–665.
6. Cuypers E, et al. (2008) Gambierol, a toxin produced by the dinoflagellate *Gambierdiscus toxicus*, is a potent blocker of voltage-gated potassium channels. *Toxicon* 51:974–983.
7. Swartz KJ (2007) Tarantula toxins interacting with voltage sensors in potassium channels. *Toxicon* 49:213–230.
8. Swartz KJ, MacKinnon R (1997) Hanatoxin modifies the gating of a voltage-dependent K^+ channel through multiple binding sites. *Neuron* 18:665–673.
9. Phillips LR, et al. (2005) Voltage-sensor activation with a tarantula toxin as cargo. *Nature* 436:857–860.
10. Herrera D, et al. (2005) A single residue in the S6 transmembrane domain governs the differential flecainide sensitivity of voltage-gated potassium channels. *Mol Pharmacol* 68:305–316.
11. Long SB, Campbell EB, MacKinnon R (2005) Crystal structure of a mammalian voltage-dependent *Shaker* family K^+ channel. *Science* 309:897–903.
12. Pathak MM, et al. (2007) Closing in on the resting state of the *Shaker* K^+ channel. *Neuron* 56:124–140.
13. Rodriguez de la Vega RC, Merino E, Becerril B, Possani LD (2003) Novel interactions between K^+ channels and scorpion toxins. *Trends Pharmacol Sci* 24:222–227.
14. Hidalgo P, MacKinnon R (1995) Revealing the architecture of a K^+ channel pore through mutant cycles with a peptide inhibitor. *Science* 268:307–310.
15. Tytgat J, Debont T, Carmeliet E, Daenens P (1995) The alpha-dendrotoxin footprint on a mammalian potassium channel. *J Biol Chem* 270:24776–24781.
16. Lenaeus MJ, Vamvouka M, Focia PJ, Gross A (2005) Structural basis of TEA blockade in a model potassium channel. *Nat Struct Mol Biol* 12:454–459.
17. Armstrong CM (1971) Interaction of tetraethylammonium ion derivatives with the potassium channels of giant axons. *J Gen Physiol* 58:413–437.
18. Decher N, Kumar P, Gonzalez T, Pirard B, Sanguinetti MC (2006) Binding site of a novel Kv1.5 blocker: A ''foot in the door'' against atrial fibrillation. *Mol Pharmacol* 70:1204–1211.
19. Snyders DJ, Knoth KM, Roberds SL, Tamkun MM (1992) Time-, voltage-, and state-dependent block by quinidine of a cloned human cardiac potassium channel. *Mol Pharmacol* 41:322–330.
20. Snyders DJ, Chaudhary AC (1996) High affinity open-channel block by dofetilide of *HERG*, expressed in a human cell line. *Mol Pharmacol* 49:949–955.
21. Eldstrom J, et al. (2007) The molecular basis of high-affinity binding of the antiarrhythmic compound vernakalant (RSD1235) to Kv1.5 channels. *Mol Pharmacol* 72:1522–1534.
22. Lee SY, MacKinnon R (2004) A membrane-access mechanism of ion channel inhibition by voltage sensor toxins from spider venom. *Nature* 430:232–235.
23. Milescu M, et al. (2007) Tarantula toxins interact with voltage sensors within lipid membranes. *J Gen Physiol* 130:497–511.
24. Trainer VL, Baden DG, Catterall WA (1994) Identification of peptide components of the brevetoxin receptor site of rat brain sodium channels. *J Biol Chem* 269:19904–19909.
25. Jeglitsch G, Rein K, Baden DG, Adams DJ (1998) Brevetoxin-3 (PbTx-3) and its derivatives modulate single tetrodotoxin-sensitive sodium channels in rat sensory neurons. *J Pharmacol Exp Ther* 284:516–525.
26. Inoue M, Hirama M, Satake M, Sugiyama K, Yasumoto T (2003) Inhibition of brevetoxin binding to the voltage-gated sodium channel by gambierol and gambieric acid-A. *Toxicon* 41:469–474.
27. Fuwa H, et al. (2004) Diverted total synthesis and biological evaluation of gambierol analogues: Elucidation of crucial structural elements for potent toxicity. *Chemistry* 10:4894–4909.
28. Heitzmann D, Warth R (2008) Physiology and pathophysiology of potassium channels in gastrointestinal epithelia. *Physiol Rev* 88:1119–1182.
29. Gutman GA, et al. (2005) International Union of Pharmacology. LIII. Nomenclature and molecular relationships of voltage-gated potassium channels. *Pharmacol Rev* 57:473–508.
30. Birinyi-Strachan LC, Gunning SJ, Lewis RJ, Nicholson GM (2005) Block of voltage-gated potassium channels by Pacific ciguatoxin-1 contributes to increased neuronal excitability in rat sensory neurons. *Toxicol Appl Pharmacol* 204:175–186.
31. Johnson HW, Majumder U, Rainier JD (2006) Total synthesis of gambierol: Subunit coupling and completion. *Chemistry* 12:1747–1753.
32. Arnold K, Bordoli L, Kopp J, Schwede T (2006) The SWISS-MODEL workspace: A web-based environment for protein structure homology modelling. *Bioinformatics* 22:195–201.
33. Humphrey W, Dalke A, Schulten K (1996) VMD: Visual molecular dynamics. *J Mol Graphics* 14:33–38.